Generation of WDM adaptive-rate pulse bursts by cascading narrow/wideband tunable optical dispersion compensators

David Sinefeld,* Yiska Fattal, and Dan M. Marom

Applied Physics Department, Hebrew University, Jerusalem 91904, Israel

**Corresponding author: sinefeld@gmail.com*

Received June 11, 2012; revised August 14, 2012; accepted September 11, 2012; posted September 12, 2012 (Doc. ID 170378); published October 11, 2012

We demonstrate passive generation of optical pulse trains with each pulse having distinct center carrier and spectra using tunable group delay (GD) staircase transfer functions. The GD steps result from opposite and equal magnitude GD slopes from narrowband and wideband tunable optical dispersion compensators. We use this technique to split the spectrum of a femtosecond pulse to a pulse burst with precise control of pulse time separation.

OCIS codes: 130.2035, 320.5540.

Chirped pulses are the basis for many signal processing systems, such as photonically assisted analog-to-digital conversion (ADC), enabling rapid sampling of an optical signal with the benefit of color component separation, effectively slowing down the optoelectronic detection speed by the wavelength parallelism factor [1]. Chirped pulses are also useful in converting an ultrafast optical signal by way of parametric wave mixing to a frequency mapped signal, performing temporal imaging and serial-to-parallel conversion [2,3]. Some applications preferably require a discrete colored pulse train such as photonic ADC [4,5], as opposed to a continuous carrier sweep. This can be achieved by a photonic spectral processor (PSP) [6,7], which uses a phase spatial light modulator (SLM), which can be used for applying different phase slopes to different spectral channels. However, adding phase slopes to the spectrum using the PSP approach results in losses which increase with the associated time delay [6], and the use of an active SLM component to generate the desired group delay (GD) function is expensive.

Our proposed method for generating a WDM pulse burst with passive components only is based on realizing a transfer function consisting of a GD staircase, by cascading a continuous chromatic dispersive (CD) element with a narrow free spectral range (FSR) WDM dispersion compensator of opposite GD slope, as shown in Fig. 1 (first reported in [8]). Here we report improved experimental results and introduce measurements of the high-speed temporal response. Continuous (or WB) CD is characterized by fixed GD slope versus wavelength, with the slope defining the CD (in ps/nm units). Finite (or NB) FSR CD has sawtooth GD versus wavelength pattern. Their cascade, when the slopes are equal in magnitude and opposite in sign, create GD stairs where the step height, ΔGD, is given by

$$\Delta\mathrm{GD}[\mathrm{ps}] = \mathrm{CD}[\mathrm{ps/nm}] \cdot \Delta\lambda[\mathrm{nm}], \tag{1}$$

where $\Delta\lambda$ is the FSR. If an ultrashort pulse traverses the staircase transfer function, it will be filtered to a burst of subpulses, each being transform-limited, delayed in time, and of contiguous spectral extent. Furthermore, if both the WB and NB CD are made tunable, then the pulse burst is also rate adaptable, with the rate being the inverse of ΔGD.

In this Letter, we demonstrate the tuning ability of the GD staircase with customized tunable optical dispersion compensator (TODC) processors, and produce for the first time WDM adaptive-rate optical pulse bursts by filtering an incident ultrashort pulse in the telecom-band.

We previously demonstrated a NB TODC, realized by translation of an arrayed waveguide grating (AWG) whose output radiates to free space [Fig. 2(a)] [9]. The AWG defines the FSR, according to the incremental length change of the waveguide arms, FSR $= \lambda/m$, where m is the AWG diffraction order and λ is the wavelength inside the waveguide. The angularly dispersed light at the output facet, $d\theta/d\lambda$, is converted to spatial dispersion with a Fourier lens, and additional phase curvature due to an offset, Δz, between the AWG output from the lens front focal plane is converted to CD according to [9,10]

$$\mathrm{CD} = \frac{2\lambda_0}{c_0}\left(\frac{d\theta}{d\lambda}\right)^2 \Delta z. \tag{2}$$

Hence, a desired CD is set by translation only, and a periodic GD sawtooth pattern is generated. We applied the same technique toward realization of a WB TODC. WB support was achieved by replacing the AWG with a bulk grating [Fig. 2(b)]. Since the bulk grating's angular dispersion is much smaller, and to eliminate

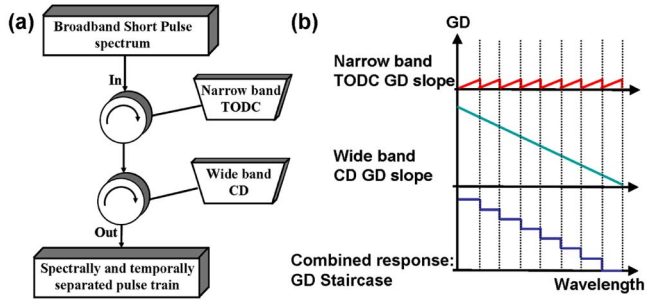

Fig. 1. (Color online) Layout of the tunable GD system: (a) System arrangement. (b) NB TODC and WB TODC GD slopes and the resultant GD staircase.

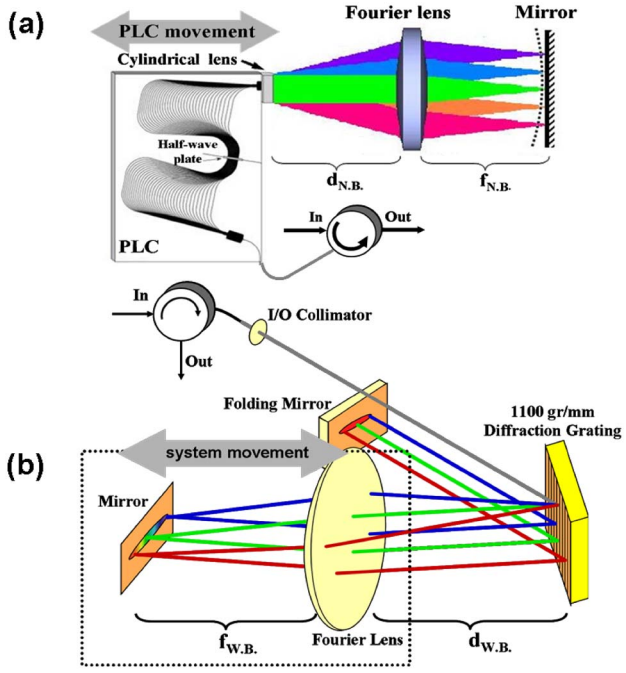

Fig. 2. (Color online) (a) NB TODC based on high resolution dispersion from an AWG. Changing the grating-lens distance, $d_{N\cdot B}$, results in quadratic spectral phase or GD slope. (b) WB TODC of similar nature with a bulk diffraction grating. The system is double-passed to maximize the CD capacity and avoid spectral narrowing.

spatiotemporal coupling effects, the system is double-passed (by reflecting off a folding mirror and experiencing four grating diffraction events). The NB TODC has a 100 GHz (0.81 nm) FSR, yielding $m \cong 1900$, with output waveguides at pitch of $p = 16$ μm, leading to angular dispersion of $d\theta/d\lambda = 120$ mrad/nm. In contrast, the WB TODC with a 1100 gr/mm grating mounted near Littrow has $d\theta/d\lambda = 5.7$ mrad/nm. Due to the CD dependence on angular dispersion squared [Eq. (2)], the WB TODC has to translate 220 times as much for an identical CD setting (including factor 2 due to double-passing WB TODC).

The elements of the NB TODC and the WB TODC were assembled on separate compact optical benches. The tunable WB CD used a Fourier lens with focal length of 500 mm, to accommodate for large grating displacements from the front focal plane. The overall optical length of the setup is approximately 4 m, since the light travels along the system four times. A circulator was used to separate the input and output light to each subsystem. The TODCs were characterized separately and jointly using a LUNA OVA (Optical Vector Analyzer). The insertion loss (IL) of each subsystem is less than 10 dB, thus the overall IL was ~18.5 dB [Fig. 3(d)]. Reduction of IL and system size can be implemented by using more efficient passive elements, such as single-mode fiber (SMF) for the WB CD generation and etalon [11] or sampled fiber bragg grating [12] based TODC for the NB response.

The tuninig ability and accuracy of the system is shown in Figs. 3 and 4. The dispersion of the WB and the NB systems was set to ±18.75 (blue) and ±50 ps/nm (green). The combination of the NB TODC GD slopes [Fig. 3(a)] with the WB TODC slopes [Fig. 3(b)] resulted

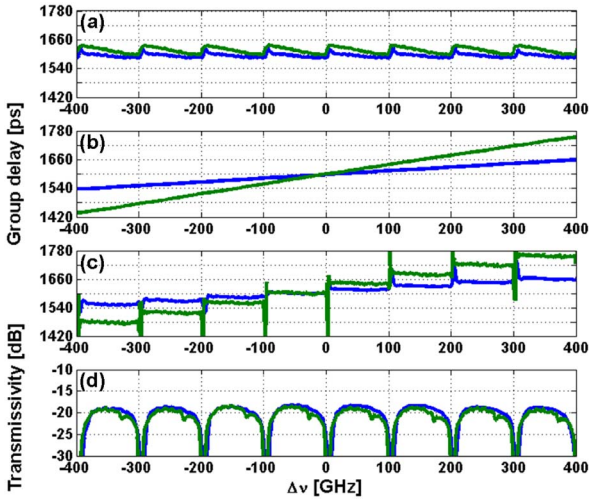

Fig. 3. (Color online) Plots of measured GD with slopes of ±18.75 ps/nm (blue) and ±50 ps/nm (green). (a) NB TODC. (b) WB TODC. (c) The combined TODC with the GD staircase pattern, with step heights of 15 ps (blue) and 40 ps (green). (d) IL of the combined TODC in both cases.

in the desired GD staircase pattern [Fig. 3(c)]. Since the NB FSR is 0.81 nm, the GD staircase step height is ~15 ps (40 ps) for GD slopes of ±18.75 ps/nm (±50 ps/nm), resulting 66.6 GHz (25 GHz) pulse bursts.

The two GD staircase patterns were used to filter ultrashort (100 fs) pulses at $\lambda_0 = 1.55$ μm from a mode-locked laser (MLL). We used Spectra Physics Tsunami + Opal MLL, with a pulse rate of 80 MHz and average power of 300 mW. Each filtered ultrashort pulse generates a finite duration WDM pulse burst. A continuous WDM pulse sampling sequence can be generated by employing a higher repetition rate MLL. The generated pulse bursts were measured with a high-speed optical sampling scope (HS-OSS) (65 GHz), having interpulse spacings of 15 and 40 ps (Fig. 4). The NB TODC has a spectral filtering bandwidth of ~60 GHz, leading to filtered, transform-limited pulses of ~17 ps duration FWHM. For the 25 GHz pulse burst, this corresponds to a pulse burst duty cycle of 0.33. For both pulse bursts, no loss degradation was observed, and the loss was

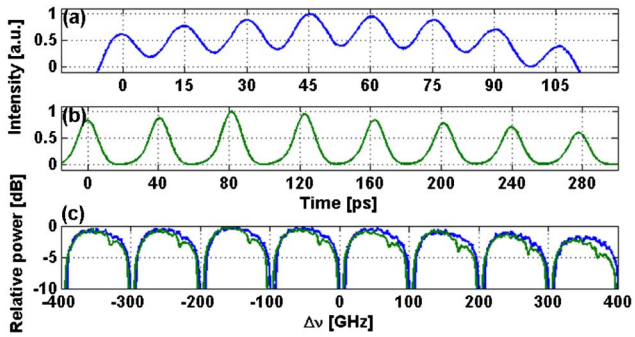

Fig. 4. (Color online) High-speed oscilloscope (HS-OSS) measurements of the WDM pulse bursts that were generated with GD system: (a) 15 ps spaced pulses. (b) 40 ps spaced pulses. (c) OSA measurement of the relative power of the filtered MLL spectrum for both 15 ps (blue) and 40 ps (green) spaced pulses.

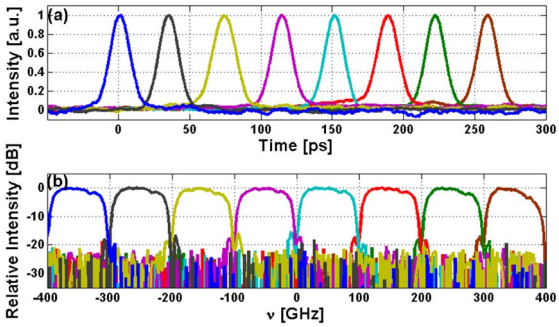

Fig. 5. (Color online) Validation experiment of unique pulse center carrier and spectrum by WDM channel filtering, and subsequent HS-OSS measurements and corresponding OSA measurements, collected and normalized for each filtered pulse separately. (a) Temporal measurements and (b) spectral measurements. The colors in (a) and (b) are matched, showing that each pulse has distinguished spectral content.

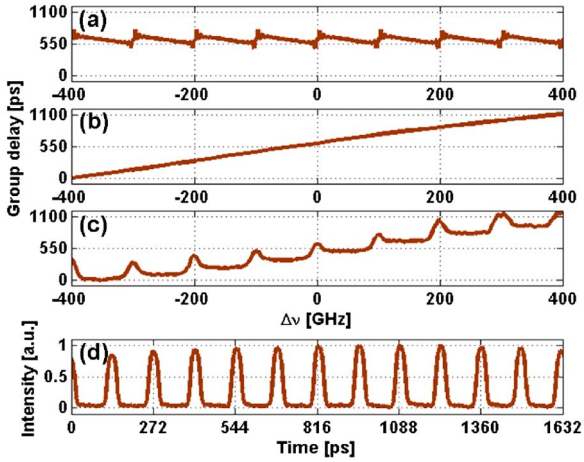

Fig. 6. (Color online) Staircase GD produced by a combination of CD from 10 km SMF and a NB TODC. (a) NB TODC with GD slope of −170 ps/nm. (b) WB TODC with GD slope of 170 ps/nm. (c) The combined setup with the resultant GD staircase pattern, with step height of 136 ps. (d) HS-OSS measurements of the WDM pulse burst.

relatively uniform along all pulses [Fig. 3(d)]. With a PSP approach [6], where each pulse is independently delayed, there will be delay-dependent losses along the spectrum. To show that the pulse burst is truly wavelength distinguishable, we used a WDM channel filter allowing the transmission of one WDM channel at a time for selecting individual pulses from the pulse burst. While keeping the time frame along the whole measurements, we performed both temporal measurements with the HS-OSS, and spectral measurement using an optical spectrum analyzer (OSA), resulting in a direct correspondence between pulse position and spectrum (Fig. 5).

Since our WB TODC is limited in its dispersion generating range to ~80 ps/nm and in bandwidth to 6.4 nm (or 8 FSR periods), due to the finite grating and lens apertures, we also demonstrated the GD staircase generation concept with a spool of 10 km SMF (Fig. 6). Since the LUNA OVA cannot measure such distances due to its limited coherence length, we used a modulation phase shift method instead, in order to characterize the GD. The SMF spool was measured to have 170 ps/nm GD slope, which was compensated by the NB TODC to give ~136 ps GD difference between adjacent channels [Fig. 6(c)] corresponding to a 7.5 GHz pulse burst with an overall IL of −15 dB. This arrangement was also measured by the HS-OSS [Fig. 6(d)]. The resulting pulse burst contains ~50 pulses having an envelope function following the spectrum of the MLL, with a ~15% duty cycle, and spanning nearly 7 ns.

In summary, we have demonstrated the transfer function of a GD staircase, capable of slicing an ultrashort pulse to a sequence of spectrally nonoverlapping transform-limited pulses using only passive components. The resultant pulse burst rate depends on the applied CD and the FSR of the TODC element, and can be made adaptive when using tunable processors as demonstrated herein. The technique is scalable toward generation of pulse bursts at rates of hundreds of gigahertz, provided the input pulse is sufficiently broadband [13] and as the FSR of the NB TODC is increased to the desired value. The timing accuracy of the technique is determined by higher-order dispersion, i.e., deviation from linearity in the GD slope. This can be ameliorated by dispersion compensation techniques. The resulting pulse burst technique is different from [14], which is not wavelength distinguishable.

The authors would like to thank Civcom for the privilege of using LUNA OVA to carry out GD measurements, U. Levy for loaning of the HS-OSS, and the Ministry of Industry Kamin program for funding.

References

1. Y. Han and B. Jalali, J. Lightwave Technol. **21**, 3085 (2003).
2. M. A. Foster, A. C. Turner, R. Salem, M. Lipson, and A. L. Gaeta, Opt. Express **15**, 12949 (2007).
3. H. C. H. Mulvad, E. Palushani, H. Hu, H. Ji, M. Lillieholm, M. Galili, A. T. Clausen, M. Pu, K. Yvind, J. M. Hvam, P. Jeppesen, and L. K. Oxenløwe, Opt. Express **19**, B825 (2011).
4. A. Yariv and R. G. M. P. Koumans, Electron. Lett. **34**, 2012 (1998).
5. J. Kim, M. J. Park, M. H. Perrott, and F. X. Kärtner, Opt. Express **16**, 16509 (2008).
6. D. Sinefeld, C. R. Doerr, and D. M. Marom, Opt. Express **19**, 14532 (2011).
7. X. Yi, L. Li, T. X. H. Huang, and R. A. Minasian, Opt. Lett. **37**, 608 (2012).
8. D. Sinefeld, Y. Fattal, and D. Marom, in *National Fiber Optic Engineers Conference*, OSA Technical Digest (Optical Society of America, 2012), paper JTh2A.3.
9. D. Sinefeld, S. Ben-Ezra, C. R. Doerr, and D. M. Marom, Opt. Lett. **36**, 1410 (2011).
10. K. Seno, N. Ooba, K. Suzuki, T. Watanabe, K. Watanabe, and S. Mino, IEEE Photon. Technol. Lett. **21**, 1701 (2009).
11. X. Shu, K. Sugden, P. Rhead, J. Mitchell, I. Felmeri, G. Lloyd, K. Byron, Z. Huang, I. Khrushchev, and I. Bennion, IEEE Photon. Technol. Lett. **15**, 1111 (2003).
12. K.-M. Feng, J.-X. Chai, V. Grubsky, D. S. Starodubov, M. I. Hayee, S. Lee, X. Jiang, A. E. Willner, and J. Feinberg, IEEE Photon. Technol. Lett. **11**, 373 (1999).
13. J. M. Dudley, G. Gentry, and S. Coen, Rev. Mod. Phys. **78**, 1135 (2006).
14. D. E. Leaird, S. Shen, A. M. Weiner, A. Sugita, S. Kamei, M. Ishii, and K. Okamoto, IEEE Photon. Technol. Lett. **13**, 221 (2001).